

Constraining the Braking Indices of Magnetars

Z. F. Gao^{1,2,*}, X.-D. Li³, N. Wang^{1 †}, J. P. Yuan¹, Q.H. Peng³, Y.J. Du⁴,

¹ Xijiang Astronomical Observatory, Chinese Academy of Sciences, 150, Science 1-Street, Urumqi, Xinjiang, 830011, China

² Key Laboratory of Radio Astronomy, Chinese Academy of Sciences, West Beijing Road, Nanjing, Jiangsu 210008, China

³ School of Astronomy and Space Science, Nanjing University, Jiangsu, 210046, China

⁴ National Space Science Center, Chinese Academy of Sciences, Beijing, 100190, China

26 January 2019

ABSTRACT

Due to the lack of long term pulsed emission in quiescence and the strong timing noise, it is impossible to directly measure the braking index n of a magnetar. Based on the estimated ages of their potentially associated supernova remnants (SNRs), we estimate the values of n of nine magnetars with SNRs, and find that they cluster in a range of $1 \sim 41$. Six magnetars have smaller braking indices of $1 < n < 3$, and we interpret them within a combination of magneto-dipole radiation and wind aided braking, while the larger braking indices of $n > 3$ for other three magnetars are attributed to the decay of external braking torque, which might be caused by magnetic field decay. We estimate the possible wind luminosities for the magnetars with $1 < n < 3$, and the dipolar magnetic field decay rates for the magnetars with $n > 3$ within the updated magneto-thermal evolution models. We point out that there could be some connections between the magnetar's anti-glitch event and its braking index, and the magnitude of n should be taken into account when explaining the event. Although the constrained range of the magnetars' braking indices is tentative, our method provides an effective way to constrain the magnetars' braking indices if the measurements of the SNRs' ages are reliable, which can be improved by future observations.

Key words: Magnetars: Supernova remnant: Winds:

1 INTRODUCTION

Pulsars are commonly recognized as magnetized neutron stars (NSs), sometimes have been argued to be quark stars (Zheng et al. 2006; Xu 2007; Lai et al. 2013). A pulsar's secular spin-down is mainly caused by its rotational energy losses due to electromagnetic radiation, particle winds, star-disk interaction, intense neutrino emission or gravitational radiation (e.g., Peng et al. 1982; Harding et al. 1999; Alpar & Baykal 2006; Chen & Li 2006). An important and measurable quantity closely related to a pulsar's rotational evolution is the braking index n , defined by assuming that the star spins down in the light of a power law

$$\dot{\Omega} = -K\Omega^n, \quad (1)$$

where Ω is the angular velocity, $\dot{\Omega}$ is the derivative of Ω , and K is a proportionality constant hiding different dependences on the star's radius, moment of inertia, magnetic field strength, and the angle between rotational and magnetic axes, etc. When the magneto-dipole radiation (MDR)

solely causes the pulsar spin-down, the braking index is predicted to be $n = 3$. Note that this constant value of $n = 3$ holds only if the torque is proportional to Ω^3 , which is the case for the magnetic torque with K keeping constant over time (Pons et al. 2012). However, in general n can vary over time because variations in any of these quantities may result in departures from this predicted value of 3.

The standard way to define the braking index is

$$n \equiv \frac{\Omega \ddot{\Omega}}{\dot{\Omega}^2} = \frac{\nu \ddot{\nu}}{\dot{\nu}^2} = 2 - \frac{P \ddot{P}}{\dot{P}^2}, \quad (2)$$

where $\ddot{\Omega}$ the second derivative of Ω , $\nu = \Omega/2\pi$ is the spin frequency and $P = 1/\nu$ the spin period (see Manchester & Taylor 1977, and references therein). Be cautious that the measured value of n strongly depends on a certain time-span, and any variation in the magnetic torque will give a time-varying $n(t)$. The braking index also tells us some simple physical expectation. For example, $n = 5$ may point to gravitational-wave-emission¹ as the dominant spin-down

¹ For a normal radio pulsar, gravitational wave radiation can be only efficient during the first minutes/hours of the life (Manchester & Taylor 1977).

* E-mail: zhifugao@xao.ac.cn

† E-mail: na.wang@xao.ac.cn

Table 1. Braking indices of 13 young radio pulsars

Source Name	n	Reference
B0531+21(Crab)	2.51(1)	Lyne et al. 1993
J0537–6910	~ -1.5	Middleditch et al. 2006
B0540–69	2.140(9)	Livingstone et al. 2007
B0833–45(Vela)	1.4(2)	Lyne et al. 1996
J1119–6127	2.91(5)	Weltevrede et al. 2011
B1509–58	2.839(1)	Lyne et al. 1996
J1734–3333	0.9(2)	Espinoza et al. 2011
J1747–2958	< 1.3	Hales et al. 2009
B1757–24	~ -1	Espinoza 2013
B1800–21	2	Espinoza 2013
B1813–1749	2	Espinoza 2013
J1835–1034	1.857(6)	Roy et al. 2012
J1846–0258	2.65(1)	Livingstone et al. 2007

mechanism, while in the case of $n = 1$, particle-wind radiation solely causes the pulsar spin down.

For the majority of pulsars, it is extraordinarily difficult to measure their stable and sensible braking indices n , from pulsar timing-fitting by using Eq.(2). The main reason has been largely attributed to the rotational irregularities, such as glitches, an abrupt increases in ν and $\dot{\nu}$ followed by relaxations (Yuan et al. 2010), and timing noise (Zhang & Xie 2013; Kutukcu & Ankaray 2014; Haskell & Melatos 2015).

By analyzing the timing irregularities for 366 non-recycled pulsars with ages $t > 10^4$ yrs, Hobbs et al. (2010) measured their braking indices and showed that they rang from -287986 to $+3624$. These large values of n strengthen our viewpoint that the characteristic age τ_c ($\tau_c = P/2\dot{P}$ assuming a constant value of $n = 3$) is a poor proxy for the true age of a pulsar. As noted in Pons et al. (2012), any small relative variation of the torque will produce large variation in n for old pulsars. Only for young radio pulsars, which spin down quickly, experience few small glitches and have low-level timing noise, and their stable and reliable braking indices have been measured, as shown in Table 1. Eleven sources have positive braking indices below the canonical value of 3.

The very small braking index of $n = 0.9 \pm 0.2$ (for PSR J1734–3333), $n \sim -1.5$ (for PSR J0537–6910), and $n \sim -1$ (for PSR B1757–24) could be consistent with the reemergence of magnetic fields after a deep submergence into the star’s crust (Muslimov & Page 1995; Ho 2011; Viganò & Pons 2012). According to the magneto-thermal evolution model proposed by Pons et al. (2012), a reemergence or a temporal rise of the crustal field, due to Ohmic dissipation and Hall drift, could in principle provide any braking-index value smaller than 3. Braking indices reaching values of $\pm 10^{4\sim 5}$ were **also** reported (Manchester et al. 2005). These observations could be contaminated by unsettled glitches or timing noise (Alpar & Baykal 2006). Other interpretations for such large $|n|$ have also been proposed (Barsukov & Tsygan 2010; Biryukov et al. 2012; Pons et al. 2012; Zhang & Xie 2012).

Anomalous X-ray pulsars (AXPs) and soft gamma repeaters (SGRs) are usually accepted as magnetars (Duncan & Thompson 1992; Thompson & Duncan 1995). They

are young NSs endowed with large surface dipolar magnetic fields. The soft X-ray emission in quiescence, bursts and flares of magnetars is supposed to be fueled by the rearrangement and decay of the superhigh internal multiple magnetic fields (e.g., Gao et al. 2011, 2012, 2013)².

It is commonly believed that pulsars, including traditional radio pulsars and magnetars, are produced in core-collapse supernova explosions. Supernova remnants (SNRs) are the expanding diffuse gaseous nebulas resulting from the explosions of massive stars. SNRs can provide direct insights into the NS progenitor models and the explosion mechanisms, and thus have been studied by many groups (e.g., Tian et al. 2007; Espinoza 2013; Zhou et al. 2013).

To date, we have obtained available information of 28 known magnetars: 14 SGRs (11 confirmed), and 14 AXPs (12 confirmed). Among these sources, only 4 transient magnetars (1E 1547.0–5408, PSR J1622–4950, SGR J1745–2900 and XTE 1810–197) are discovered to emit radio waves during their outbursts. With the exception of SGR 0418+5729, all known Galactic magnetars lie within 2° of the Galactic Plane, consistent with a population of young objects, see in “The McGill Magnetar Catalog”. An online version of the catalog is located at the web site <http://www.physics.mcgill.ca/~pulsar/magnetar/main.html>, (Olausen & Kaspi 2014).

The study of the braking indices of magnetars can provide a wealth of information about the magneto–thermal evolution, the spin evolution, and the radio–emission mechanism of these objects. However, due to the lack of quiescent radio emission and strong timing noise, we have not yet measured the values of n for magnetars. Observations hint that some magnetars have associations with clusters of massive stars. In the recent works by Tendulkar et al. (2012, 2013), assuming that SGR 1806–20 and SGR 1900+14 were born in star clusters, the authors firstly measured the kinetic ages of these two sources, and then estimated their braking indices.

Although the braking indices of magnetars have been investigated by some authors (e.g., Hobbs et al. 2010; Tendulkar et al. 2012; Magalhaes et al. 2012), the work of specifically constraining the braking index of a magnetar has not appeared so far. In this paper, we try to constrain the braking indices of magnetars from the ages of their SNRs. In Sec. 2, we describe the potential magnetar/SNR associations. In Sec. 3, we present constrained values of n for nine magnetars with SNRs, and possible explanations. We introduce one potential application of our model in Sec. 4, and summarize in Sec. 5.

2 POTENTIAL MAGNETAR/SNR ASSOCIATIONS

It was predicted that about 10% of Galactic supernova explosions may lead to magnetars (Kouveliotou et al. 1994). Observations hint that about one third of the magnetars are likely to be associated with SNRs, suggestive of an origin of massive star explosions. Currently, the remnants ages are

² The internal magnetic field of a magnetar could be a mixture of toroidal and poloidal magnetic fields, and the toroidal component dominates (Mereghetti 2008; Olausen & Kaspi 2014).

estimated based on the measurements of the shock velocities, and/or the X-ray temperatures and/or other quantities. The SNR evolution can be schematically divided into three successive phases:

(i) An ejecta-dominated phase. A shock wave created by supernova explosion has a free expansion velocity of $5000 \sim 10000 \text{ km s}^{-1}$ (Woltjer 1972).

(ii) A Sedov-Taylor phase. The radiative losses from a SNR in this adiabatic expansion stage are dynamically insignificant and can be neglected.

(iii) A radiation-dominated snowplow phase. When the temperature drops below about 10^6 K , radiation becomes important, and energy is lost mainly through radiation. This phase ends with the dispersion of the envelope as its velocity falls to about 9 km s^{-1} (Bandiera 1984).

Sedov (1959) showed that there is a self-similar solution for the adiabatic expansion phase (i.e., the structure of a SNR keeps constant within this stage), and firstly applied this solution to estimate the age of SNRs in this phase, i.e., the Sedov age. The Sedov age estimates rely on many assumptions, but ultimately on the SNR size and the SNR temperature. If a SNR is too young (when the expansion is free), or too old (when radiation energy losses brake the expansion), the Sedov expansion is no longer applicable.

Many authors (e.g., Ostriker & McKee 1988; Truelove & McKee 1999; Gaensler & Slane 2006) subsequently investigated the Sedov ages of SNRs. Based on *XMM-Newton* observations, Vink & Kuiper (2006) employed the Sedov evolution, and estimated the supernova explosion energies E , and SNR ages t_{SNR} by

$$2.026Et_{\text{SNR}}^2 = R_s^5 \rho_0, \quad (3)$$

where ρ_0 is the interstellar medium density, and R_s the shock radius, which approximates to the SNR radius R_{SNR} . The shock velocity v_s can be obtained by

$$kT = \frac{3}{16} \times 0.63m_p v_s^2, \quad (4)$$

where T is the post-shock plasma temperature, m_p is the proton mass, and the number 0.63 gives the mean particle mass in units of m_p for a fully ionized plasma. From Eq.(4), we can obtain the value of v_s , given the measured temperature T . The age of the remnant can be estimated from the shock velocity similarity solution

$$v_s = \dot{R}_{\text{SNR}} = \frac{2R_{\text{SNR}}}{5t_{\text{SNR}}}. \quad (5)$$

Inserting Eq.(4) into Eq.(5), we get a convenient expression

$$t_{\text{SNR}} \approx 435 \times R_{\text{SNR}} T^{-1/2} \text{ yrs}, \quad (6)$$

where R_{SNR} and T are in units of pc and keV, respectively³. With respect to the potential magnetar/SNR associations, Gaensler (2004) proposed important criteria, which include evidence for interaction, consistent distances/ages, inferred transverse velocity, proper motion and the probability of random alignment. However, due to the observational limit, these criteria cannot always be applicable. The judgement as to whether a potential magnetar/SNR association meets

these requirements ultimately depends on observational evidences. As pointed out by Gaensler (2004), one basic indication of the likelihood of an association is the chance coincidence probability between a magnetar and its host SNR.

In the following, we briefly review the measured and derived parameters for the nine magnetars and their associated SNRs. All these SNRs have kinetic distances derived from their associations with other objects (e.g., molecular clouds) having known distances.

(i) 1E 1841–045 (hereafter 1E 1841) The error box of this AXP lies within the SNR Kes 73 (G27.4+0.0), which is nearly circular in X-rays with an angular diameter of $\theta = 4.5'$ (Helfand et al. 1994; Gotthelf & Vasisht 1997). The probability of chance alignment was estimated to be 1×10^{-4} for this association (Vasisht & Gotthelf 1997; Gaensler 2004). Using the galactic circular rotation model, Tian & Leahy (2008) gave a range of revised distance to Kes 73 about $7.5 \sim 9.8 \text{ kpc}$, which implies a shock radius $R_{\text{SNR}} \approx 4.9 \sim 6.4 \text{ pc}$. Then the Sedov age of Kes 73 was estimated to be $500 \sim 1000 \text{ yrs}$ for standard explosion energy ($E = 10^{51} \text{ erg}$) and interstellar medium (ISM) density $n=1 \text{ cm}^{-3}$ (Tian & Leahy 2008).

(ii) SGR 0526–66 (hereafter SGR 0526) This SGR could be physically associated with the remnant N49 (Evans et al. 1980) located in the Large Magellanic Cloud (LMC) at a distance of 50 kpc and interacting with a molecular cloud. The deep *Chandra* observation indicated the gas temperature in the shell region to be $T=0.57 \text{ keV}$ for N49 (Park et al. 2012). Assume an angular distance of $35''$ between the Shell region and the geometric center of N49, the SNR radius is estimated to be 8.5 pc, then the Sedov age of the SNR is 4800 yrs (Park et al. 2012). However, the association between this SGR and N49 is controversial (e.g., Gaensler et al. 2001; Klose et al. 2004; Badenes et al. 2009), and more evidence is needed to testify this potential association.

(iii) SGR 1627–41 (hereafter SGR 1627) This SGR is associated with the G337.0–0.1 (Hurley et al. 1999), and is located on the edge of massive molecular clouds. The angular size (radius of $\sim 45''$) of G337.0–0.1 implies a radius of 2.4 pc at a distance of 11.0 kpc (Sarma et al. 1997). The spurious probability of the SGR/SNR association was estimated to $\sim 5\%$ (Smith et al. 1999). The age of the SNR was estimated to be 5000 yrs based on the Swedish-ESO Submillimeter Telescope observations (Corbel et al. 1999).

(iv) SGR 0501+4516 (hereafter SGR 0501) This SGR could be associated with SNR HB9 (also known as G160.9+2.6)(Gaensler & Chatterjee 2008) with an angular diameter of $128'$ (Leahy & Aschenbach 1995), but this association is not confirmed by observations (Barthelmy et al. 2008). The centrally brighten X-ray emission with $T \sim 0.82 \text{ keV}$ from HB9 can be explained by self-similar evolution in a cloudy interstellar medium proposed by White & Long (1991) (WL91). Applying the WL91 evaporative cloud model, Leahy & Aschenbach (1995) (LA95) gave a distance of $d = 1.5 \text{ kpc}$ (corresponding to $R_{\text{SNR}} \sim 28 \text{ pc}$) and an age of 7700 yrs for the SNR. Based on the H I absorption measurement, Leahy & Tian (2007) (LA07) obtained a distance of $d = 0.8 \pm 0.4 \text{ kpc}$ (the mean radius is 15 pc at $d = 0.8 \text{ kpc}$), and an age of $4000 \sim 7000 \text{ yrs}$ for the SNR within WL91 evaporative cloud model. In the following, we simultaneously consider both the results of LA95 and LT07, i.e., the distance is

³ The propagated error of R_{SNR} is given by $\Delta t_{\text{SNR}} = 435 \times (\frac{\Delta^2 R_{\text{SNR}}}{T} + \frac{R_{\text{SNR}}^2 \Delta^2 T}{4T^3})^{1/2} \text{ yrs}$.

assumed to be $0.4 \sim 1.5$ kpc, and the age for the SNR varies between 4000 and 7700 yrs.

(v) PSR J1622–4950 (hereafter PSR J1622) The positional coincidence of this AXP with the center of G333.9+0.1 with an angular diameter about $12'$ suggests a possible magnetar/SNR association (Anderson et al. 2012). G333.9+0.1 has a radius of 18 pc at the distance of 9 kpc, and is in a low density medium, suggesting the Sedov-Taylor expansion. (Anderson et al. 2012). Since no X-ray emission was detected from the SNR in the *XMM-Newton* observation (Anderson et al. 2012), the upper limit on the count-rate was estimated as $0.04 \text{ counts s}^{-1}$ utilizing standard errors and roughly accounting (Romer et al. 2001). Assuming a thin-shell morphology and the Sedov-Taylor solution (Sedov 1946, 1959; Taylor 1950), the upper limit on the count-rate implies an upper limit on the preshock ambient density to be $n_0 = 0.05 \text{ cm}^{-3}$ for an explosion energy of 10^{51} erg. Then the Sedov-Taylor upper-limit for the SNR age was estimated to be 6 kyrs from this value (Anderson et al. 2012).

(vi) 1E 2259+586 (hereafter 1E 2259) This AXP lies within $4'$ of the geometric center of CTB 109 (Fahlman & Gregory 1981) with an angular radius of 18.5 ± 1.0 as estimated from the *XMM-Newton* EPIC images by Sasaki et al (2004). The probability of chance alignment is about 10^{-4} for this association (Gaensler 2004). There are some more recent estimates of the distance to CTB 109 and the AXP. Kothes & Foster (2012) collected all the observational limits of the distance (Kothes et al. 2002; Durant & van Kerkwijk 2006; Tian et al. 2010), and estimated a consensus distance of 3.2 ± 0.2 kpc to CTB 109, which places the SNR inside the Perseus spiral arm of the Milky Way. Castro et al. (2012) reported the detection of a GeV source with *Fermi* at the position of CTB 109. By simulating in the CR(cosmic rays)-Hydro-NEI (nonequilibrium ionization) model of Ellison et al.(2007), Castro et al. (2012) derived an age of the SNR to be $8.5 - 15$ kyrs, which is superior to the previous age estimates. Based on the *Chandra* data and the Sedov-Taylor solution, Sasaki et al. (2013) estimated an age of $10 \sim 20$ kyr for the SNR from a two-component model for the X-ray spectrum. Sasaki et al. (2013) also concluded that their (new) *Chandra* study is consistent with the *Fermi* results by Castro et al. (2012).

(vii) CXOU J171405.07–381031 (hereafter CXOU J1714) Halpern & Gotthelf (2010a) firstly suggested an association of this AXP with CTB 37B having a size of $17'$ (see the SNR Catalog⁴), and a distance of 10.2 ± 3.5 kpc, Caswell et al. 1975). This association has been confirmed by the period-derivative measurements by Sato et al. (2010) and Halpern & Gotthelf (2010b). Horvath & Allen (2011) gave an extensive review of this association and the SNR age. Clark & Stephenson (1975) obtained age estimates for both CTB 37A and CTB 37B of ~ 1500 yrs, and claimed that either source could be SN 393. Such an association is possible, but the SNRs may be considerably older (Downes 1984). Assuming an electron-ion equilibrium, Aharonian et al. (2008) gave a Sedov age of ~ 4900 yrs for CTB 37B. The inferred age for the SNR may be decreased to ~ 2700 yrs due to a higher ion temperature and efficient cosmic ray acceleration (Aharonian et al. 2008). Note that the

electron-ion equilibrium is usually not achieved in young SNRs. By introducing “magnetar-driven” injected energy, Horvath & Allen 2011 obtained an age of ~ 3200 yrs (see Fig. 1 in their work) for CTB 37B, but the explosion energy and the ISM density were always fixed to be 10^{51} erg and 1 cm^{-3} , respectively. Based on the *Suzaku* observations, Nakamura et al. (2009) obtained an ionization age of the thermal plasma associated with CTB 37B as 650_{-300}^{+2500} yrs, which is consistent with the tentative identification of the SNR with SN 393.

(viii) Swift J1834.9–0846 (hereafter Swift J1834) This transient magnetar is located at the center of the radio SNR W41 and the TeV source HSS J1844–087 (Kargaltsev et al. 2012). Such a central location of Swift J1834.9–0846 certainly supports the association between this SGR with W41. HI observations from the VLA Galactic Plane Survey gave a close distance of 4 ± 0.2 kpc, and an average radius $\sim 19 \pm 1$ pc for W41 (Tian et al. 2007). The authors estimated an age of ~ 60 kyr, using a Sedov model with $E \sim 0.75 \times 10^{51}$ erg, and an age of ~ 200 kyrs from complete cooling expansion (Cox 1972).

(ix) 1E 1547–5408 (hereafter 1E 1547) This AXP lies within $30''$ of the center of G327.24–0.13 with a size of $5'$ in radio (see in the SNR Catalog). The physical association of these two sources was firstly proposed by Gelfand & Gaensler (2007), and was established by other observations (e.g., Joseph et al. 2007; Vink & Bamba 2009). The distance to the SNR is quite uncertain. Assume the Galactic free electron density model (Cordes & Lazio 2002), a rough DM (dispersion-measurement) distance of 9 kpc was derived by Camilo et al. (2007), but note that this model is known to have an average uncertainty of $\sim 30\%$, which is likely much larger for individual objects (Tiengo et al. 2010). By associating 1E 1547/G327.24–0.13 with a large star-forming complex in the Scutum-Crux spiral arm, Gelfand & Gaensler (2007) obtained a distance estimate of $3.9 \sim 4.5$ kpc for the SNR. Compatible with the distance estimate by Gelfand & Gaensler (2007), Tiengo et al. (2010) gave a more likely value of $d \sim 3.91 \pm 0.07$ kpc from model-dependent interstellar dust-scattering studies. Here the age of G327.24–0.13 can be estimated as follows: The observed radio size of $\sim 5'$ (see the SNR Catalog) implies a radius of $R_{\text{SNR}} = 2.84(5)$ pc at $d = 3.91 \pm 0.07$ kpc. The X-ray spectra of 1E 1547 in both quiescence and outbursts are dominated by a black-body component with $T = 0.4 \sim 0.5$ keV, and a less Comptonized component (Gelfand & Gaensler 2007). Inserting the values of T and R_{SNR} into Eq. (6) yields an age of 1.84 ± 0.19 kyrs for the SNR.

(x) In addition, the transient magnetar AX J1845.0–0258 lies with the $5'$ diameter SNR G29.6+0.1, and the probability of chance alignment between the source and the SNR is shown to be 1.6×10^{-3} (Gaensler et al. 1999). However, due to a long-term burst behaviors, there is a lack of period derivative or dipole magnetic field for AX J1845.0–0258, so we cannot estimate its braking index. The newly identified magnetar SGR 1935+2154 was proposed to be coincident with the Galactic SNR G57.2+0.8 (Gaensler et al. 2014; Sun et al. 2011). To date, no reliable age or distance estimate is available for G57.2+0.8, and for the evaluation of the braking index of SGR 1935+2154. Thus, these two magnetars will not be considered in the following.

⁴ at <http://www.physics.umanitoba.ca/snr/SNRcat/>

Table 2. Persistent parameters for nine magnetars and their SNRs. Column one to ten are source name, spin period, spin-period derivative, surface dipole magnetic field, characteristic age, associated SNR, SNR distance, SNR radius, SNR age and reference, respectively. Data in Columns one to six are cited from Table 1 of McGill SGR/AXP Online Catalogue, up to Feb. 6, 2015. Data in Columns seven to ten are mainly cited from the SNR Catalog at <http://www.physics.umanitoba.ca/snr/SNRcat/> and from the Coolers Catalog at <http://www.neutronstarcooling.info/references.html>. In case where the timing properties vary with either phase or time, or there exists multiple recently measured values, the entries are marked with an asterisk (*) and compiled separately in Table 3.

Name	P (s)	\dot{P} 10^{-11} s/s	B_d 10^{14} G	τ_c kyrs	SNR	d_{SNR} kpc	R_{SNR} pc	t_{SNR} kyrs	Ref.
1E 1841	11.788978(1)	4.092(15)	7.0	4.6	Kes73	7.5~9.8	4.9~6.4	0.75±0.25	[1-3]
SGR 0526*	8.0544(2)	3.8(1)	5.60(7)	3.36(9)	N49	50	8.5	4.8	[4-5]
SGR 1627	2.594578(6)	1.9(4)	2.25(9)	2.2(5)	G337.0-0.1	11.0	2.4	5.0	[6-8]
SGR 0501	5.76209695(1)	0.594(2)	1.9	15	HB9	0.4~1.5	7.5~28	5.85±1.85	[9-11]
PSR J1622*	4.3261(1)	1.7(1)	2.74(8)	4.0(2)	G333.9+0.0	9	18	< 6.0	[12]
1E 2259	6.9790427250(15)	0.048369(6)	0.59	230	CTB 109	3.0~3.4 [†]	15~17 [†]	15±5	[13-15]
CXOU J1714*	3.825352(4)	6.40(5)	5.0	0.95(1)	CTB 37B	10.2	25.2	1.75±1.4	[16-18]
Swift J1834	2.4823018(1)	0.796(12)	1.42(1)	4.9	W41	3.8~4.2	18~20	130±70	[19-20]
1E 1547*	2.0721255(1)	4.77	3.2	0.69	G327.24-0.13	3.84~3.98	2.79~2.89	1.84±0.19	[21-22]

Footnotes:[†] In Sasaki et al. 2013, a very close value of $d = 2.9 \sim 3.5$ kpc was adopted, because the distance to the density peak of H I associated with arm was permitted to vary between 2.9 kpc and 3.6 kpc, although the distance to the SNR is mainly similar at 3.2 kpc, according to Kothes & Foster 2012. Refs: [1] Helfand et al. 1994 [2] Gotthelf & Vasisht 1997 [3] Tian & Leahy 2008 [4] Evans et al. 1980 [5] Park et al. 2012 [6] Sarma et al. 1997 [7] Hurley et al. 1999 [8] Corbel et al. 1999 [9] Gaensler & Chatterjee 2008 [10] Leahy & Aschenbach 1995 [11] Leahy & Tian 2007 [12] Anderson et al. 2012 [13] Kothes et al. 2002 [14] Kothes & Foster 2012 [15] Sasaki et al. 2013 [16] Caswell et al. 1975 [17] Aharonian et al. 2008 [18] Nakamura et al. 2009 [19] Tian et al. 2007 [20] Kargaltsev et al. 2012 [21] Gelfand & Gaensler 2007 [22] Tiengo et al. 2010

Table 3. Variable or alternative values of persistent parameters for four magnetars with SNRs. All data are cited from Table 2 of McGill SGR/AXP Online Catalogue at <http://www.physics.mcgill.ca/~pulsar/magnetar/table2.html>, up to Jan 10, 2015.

Name	P (s)	\dot{P} 10^{-11} s/s	B_d 10^{14} G	τ_c kyrs
SGR 0526	8.0470(2)	6.5(5)	7.3(3)	2.0(1)
PSR J1622	4.3261(1)	0.94-1.94	2.5(4)	5(2).5
CXOU J1714	3.823056(18)	5.88(8)	4.80(4)	1.03(1)
---	3.824936(17)	10.5(5)	6.4(1)	0.58(3)
1E 1547	2.06983302(4)	2.318(5)	2.2	1.4
---	2.06983302(4)	2.35-3.16	2.4(2)	1.2(2)
---	2.0721255(1)	2.66-9.78	3.5(1.1)	0.78(34)

Now, we list the parameters for nine magnetars and their SNRs. Apart from G273.24-0.13, all the SNRs in Table 2 have published age estimates. Among these objects, a few SNRs have several possible values of t_{SNR} , measured with different methods at different times, we select the age t_{SNR} that is the latest and most reliable (e.g., $t_{\text{SNR}} \sim (15 \pm 5)$ kyr for CTB 109, as shown in Table 2). For convenience, we denote each SNR age (t_{SNR}) in the same form of “main value + age error”, where the age error follows a normal distribution. With the exception of SNR W41 ($t_{\text{SNR}} \sim 130 \pm 70$ kyrs), all the ages of the magnetar SNRs are mainly distributed within a rather narrow range of 1 ~ 20 kyrs.

3 CONSTRAINING MAGNETAR BRAKING INDICES

3.1 Constrained values of n for magnetars

Since the characteristic age of a NS is not a good age-indicator, the true age t_T can be estimated as

$$t = \frac{P}{(n-1)\dot{P}} \left[1 - \left(\frac{P_i}{P} \right)^{n-1} \right] \quad (n \neq 1),$$

$$t = 2\tau_c \ln \left(\frac{P}{P_i} \right) \quad (n = 1), \quad (7)$$

given a constant braking index n , where t is the inferred age, and P_i is the initial spin period at $t = 0$ (e.g., Manchester et al. 1985; Livingstone et al. 2011). A varying n will make any analytical expression of the true age of a NS impossible. Suppose, if n increases (or decreases) with time, the pulsar true age may be greater (or lower) than the inferred age t in Eq. (7) (especially for old pulsars, the true age may be significantly lower than the inferred age).

In order to obtain the constrained values of n for magnetars, we make the following three assumptions:

(i) Firstly, we assume that a NS’s braking index keeps constant since its birth. This is a strong necessary assumption when estimating the age of a very young NS. In deed, one cannot derive an analytical expression, as Eq. (7), to estimate the age of a NS, if we consider either K or n in Eq. (1) is a time-dependent quantity. The measured braking index is obviously influenced by the variation in the braking torque during the observational intervals. Nevertheless, the derived braking index can provide useful constraints on the realistic one.

(ii) Secondly, we assume that the age of a SNR is the age of a NS. Zhang & Xie (2012) suggested that the physically meaningful criterion to estimate the true age of a NS is the NS/SNR association. This suggestion is surely in the same way applicable to magnetars with host SNRs.

Table 4. Constrained values of n for the nine magnetars with SNRs. The alternative braking indices are marked with an asterisk(*), and calculated from data in Table 4.

Source	n	Timing Reference.
1E 1841	13.181 ± 4.060	Dib & Kaspi 2014
SGR 0526	2.400 ± 0.037	Tiengo et al. 2009
---	$1.818 \pm 0.063^*$	Kulkarni et al. 2003
SGR 1627	1.866 ± 0.182	Espinoza et al. 2009a,b
SGR 0501	6.258 ± 1.663	GögüS et al. 2010
PSR J1622	$>2.345 \pm 0.079$	Levin et al. 2010
---	$>2.588 \pm 0.551^*$	Levin et al. 2010
1E 2259	31.50 ± 10.17	Dib & Kaspi 2014
CXOU J1714	2.083 ± 0.866	Sato et al. 2010
---	$2.178 \pm 0.943^*$	Halpern & Gotthelf 2010b
---	$1.660 \pm 0.529^*$	Halpern & Gotthelf 2010b
Swift J1834	1.076 ± 0.041	Kargaltsev et al. 2012
1E 1547	1.749 ± 0.081	Dib et al. 2012
---	$2.539 \pm 0.159^*$	Camilo et al. 2007
---	$2.292 \pm 0.230^*$	Camilo et al. 2007
---	$1.574 \pm 0.334^*$	Dib et al. 2012

(iii) Finally, we assume that the initial spin-period of a magnetar is far less than the current spin-period, i.e., $P_i \ll P$, because magnetars are supposed to be formed from rapidly rotating NSs (e.g. Duncan & Thompson 1992; Thompson & Duncan 1996).

Base on the above assumptions, the inferred age in Eq. (7) can be estimated as

$$t \approx \frac{P}{(n-1)\dot{P}} = -\frac{\nu}{(n-1)\dot{\nu}}, \quad (8)$$

for $\nu_i \gg \nu$. It should be noted it is the upper limit of characteristic age due to an approximation in Eq. (7). Inserting the relation $t = t_{\text{SNR}}$ into Eq. (8) gives

$$n \approx 1 - \frac{\nu}{\dot{\nu}t_{\text{SNR}}} = 1 + \frac{P}{\dot{P}t_{\text{SNR}}}. \quad (9)$$

We can calculate the values of n for nine magnetars with SNRs by combining the data in Tables 2 and 3 with Eq. (9), which are presented in Table 4. Since the first term in the right side of Eq. (9) is a constant, the error of n is solely determined by the variations of $\frac{\nu}{\dot{\nu}t_{\text{SNR}}}$ (or of $\frac{P}{\dot{P}t_{\text{SNR}}}$), the second term in the right side of Eq. (9), and the standard error Δn of n can be expressed as the form of a standard propagated error⁵. From Table 4, all the values of n deviate from 1 and 3. Six magnetars have smaller braking indices, $1 < n < 3$, while the other three have larger braking indices $n > 3$, which imply that neither pure PWR model nor pure MDR model can account for the actual braking of magnetars. In order to investigate the relation of τ_c and t_{SNR} , we plot $\text{Log}_{10}(t_{\text{SNR}}/\tau_c)$ versus $\text{Log}_{10}B$ for nine magnetars in Fig. 1.

In Fig. 1, magnetars with $n > 3$ are on the left of the dashed line whereas those with $1 < n < 3$ are on

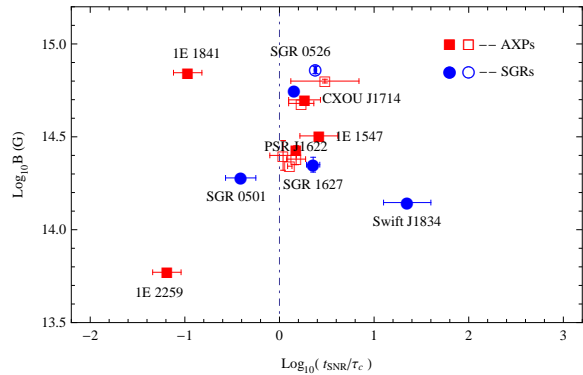


Figure 1. $\text{Log}_{10}(t_{\text{SNR}}/\tau_c)$ versus $\text{Log}_{10}B$. The dot-dashed line corresponds to $t_{\text{SNR}} = \tau_c$. Blue circles and red squares represent SGRs and AXPs, respectively. Data for empty circles and squares are from Table 3. For some sources (e.g., SGR 1627), the errors in data-points are smaller than the size of the symbols.

the right. The large discrepancy between t_{SNR} and τ_c of a magnetar can be naturally explained as follows: Inserting $P/\dot{P} = -\nu/\dot{\nu} = 2\tau_c$ into Eq. (9) gives $\tau_c/t_{\text{SNR}} = (n-1)/2$; if $n > 3$, then $\tau_c > t_{\text{SNR}}$, and a magnetar looks “older” than its true age (e.g., 1E 1841). In this case, the larger the braking index is, the larger the disparity between τ_c and t_{SNR} , as illustrated by 1E 2259. If $1 < n < 3$, then $\tau_c < t_{\text{SNR}}$, and a magnetar appear “younger” than it is, the smaller the braking index is, the larger the age-disparity.

3.2 Case of $n > 3$

The influence of the magnetic field evolution on the braking indices of radio-pulsars has been well investigated in previous studies (e.g., Geppert & Rheinhardt 2002; Aguilera et al. 2008; Pons & Geppert 2007; Pons et al. 2009; Viganò & Pons 2012; Viganò et al. 2012). In this subsection, we focus on three high braking indices ($n = 31.50 \pm 10.17$, 13.181 ± 4.060 and 6.258 ± 1.663 for 1E 2259, 1E 1841 and SGR 0501, respectively). In order to explain why the three magnetars possess large braking indices, we consider the influences of crust magnetic field decay on a magnetar’s spin-down, and refer to the works of Pons et al (2009) and Viganò et al. (2013).

According to Pons et al.(2012), the spin evolution of an isolated NS is dominated by the magnetic field anchored to the star’s solid crust, and a varying crustal magnetic field yields the braking index

$$n = 3 - 4 \frac{\dot{B}_d}{B_d} \frac{\nu}{\dot{\nu}} = 3 - 4 \frac{\dot{B}_p}{B_p} \frac{\nu}{\dot{\nu}} = 3 - 4 \frac{\tau_c}{\tau_B}, \quad (10)$$

where B_d is the surface dipole magnetic field, $B_p = 2B_d$ is the surface magnetic field at the pole, and $\tau_B = B_p/\dot{B}_p = B_d/\dot{B}_d$ is the timescale on which the dipole component of the magnetic field evolves. From Eq.(10), a decreasing surface dipole magnetic field, B_d , results in a decaying dipole braking torque, then the effective braking index increases to a high value of $n > 3$.

In order to reconcile the measured high braking indices for three magnetars with their (estimated) surface field decaying-rates, it is necessary to introduce the Hall induction equation describing the evolution of crust magnetic field

⁵ There is a relation between Δn and $\Delta\left(\frac{\nu}{\dot{\nu}t_{\text{SNR}}}\right)$, $|\Delta n| = \left|\Delta\left(\frac{\nu}{\dot{\nu}t_{\text{SNR}}}\right)\right| = \left[\left(\frac{\Delta\nu}{\dot{\nu}t_{\text{SNR}}}\right)^2 + \left(\frac{\nu\Delta t_{\text{SNR}}}{\dot{\nu}t_{\text{SNR}}^2}\right)^2 + \left(\frac{\nu\Delta\dot{\nu}}{\dot{\nu}^2 t_{\text{SNR}}}\right)^2\right]^{1/2}$.

in the following form:

$$\frac{\partial \vec{B}}{\partial t} = -\nabla \times \left[\frac{c^2}{4\pi\sigma} \nabla \times (e^\nu \vec{B}) + \frac{c}{4\pi en_e} [\nabla \times (e^\nu \vec{B})] \times \vec{B} \right], \quad (11)$$

where σ is the electric conductivity parallel to the magnetic field, e^ν is the relativistic redshift correction, n_e is the number of electrons per unit volume, and e the electron charge. On the right-hand side, the first and second terms account for Ohmic dissipation and Hall effect (which redistributes the energy of the crustal magnetic field), respectively. As to the above differential equation, Aguilera et al. (2008) presented an analytic solution

$$\frac{dB_p}{dt} = -\frac{B_p}{\tau_{\text{Ohm}}} - \frac{1}{B_p^i} \frac{B_p^2}{\tau_{\text{Hall}}}, \quad (12)$$

where τ_{Ohm} is the Ohmic dissipation timescale, and τ_{Hall} is the Hall timescale corresponding to an initial magnetic field strength B_p^i . During a NS's early magneto-thermal evolution stage, corresponding to the crust temperature $T \geq 10^8$ K, the average value of τ_{Ohm} in the crust is about 1 Myr (Pons & Geppert 2007). Since both the magnetic field strength and the density vary over many orders of magnitude in NSs' crusts, the average Hall timescale is roughly restricted as $\tau_{\text{Hall}} \sim \tau_{\text{Ohm}} / (1 - 10) B_{13}$, where B_{13} is the dipole magnetic field at the pole in units of 10^{13} G (Pons & Geppert 2007). We choose $\tau_{\text{Hall}} \sim 10^4 - 5 \times 10^5$ yrs, similar as in Viganò et al. (2013), and $\tau_{\text{Ohm}} \sim 10^6$ yrs for the three magnetars.

To estimate the values of B_p for the three magnetars, we refer to Viganò et al. (2013):

(i) By introducing the state-of-the-art kinetic coefficients and considering the important effect of the Hall term, Viganò et al. (2013) presented the updated results of 2D simulations of the NS magneto-thermal evolution, and compared their results with a data sample of 40 sources including magnetars 1E 2259, 1E 1841 and SGR 0501. It was found that by only changing the initial magnetic fields, masses and envelope compositions of the NSs, the phenomenological diversity of magnetars, high-B radio-pulsars, and isolated nearby NSs can be well explained in their theoretical models.

(ii) Comparing the cooling curves with iron envelopes for $B_p^i = 10^{15}$ G, 1E 1841 and SGR 0501 could be born with even higher magnetic field of a few 10^{15} G, which can provide a strong hard X-ray (20–200 keV) emission with a total luminosity $\sim 10^{36}$ erg s $^{-1}$ (Viganò et al. 2013).

(iii) Comparing the cooling curves for the group of NSs with $B_p^i \sim 1 - 5 \times 10^{14}$ G suggests that 1E 2259 may be born with $B_p^i \sim 3 \times 10^{14}$ G, needed to reconcile the observed timing properties and the persistent soft X-ray luminosity.

According to the above arguments, we assume $B_p^i = 3.0 \times 10^{15}$ G for 1E 1841 and SGR 0501, and $B_p^i \sim 3 \times 10^{14}$ G for 1E 2259. Inserting the values of B_p^i , B_p , τ_{Ohm} , and τ_{Hall} into Eq. (12), we obtain the estimated values of the surface magnetic field decaying-rates, $dB_p/dt = 2dB_d/dt = -(9.6 \times 10^8 \sim 4.8 \times 10^9)$, $-(1.5 \times 10^9 \sim 7.6 \times 10^{10})$, and $-(9.4 \times 10^8 \sim 4.7 \times 10^9)$ G yr $^{-1}$ for SGR 0501, 1E 1841, and 1E 2259, respectively.

Assuming the surface dipolar field decay is the only factor influencing magnetar braking indices, by combining the values of dB_p/dt with Eq. (11), we obtain the values of braking indices of $n \sim 3.2 - 4.5$ for SGR 0501, $n \sim 3.1 - 4.0$ for

1E 1841, and $n \sim 10.3 - 39.6$ for 1E 2259, which are comparable to the measured values of n for these three magnetars in the magnitude (see in Table 4).

Since magnetars are strong timing-noise sources, we cannot exclude the possibility of the decay of the magnetospheric braking torque, which can also result in larger magnetar braking indices of $n > 3$, besides the decay of the crustal magnetic field itself. Now we discuss the spin-down evolution for the three sources. SGR 0501 was firstly discovered by the Swift γ -ray observatory (Barthelmy et al. 2008). From the *RXTE/PCA*, *Swift/XRT*, *Chandra/ACIS-S*, and *XMM-Newton/PN* observations spanning a short range of MJD 54700–54950, its magnitude of $\dot{\nu}$ decreased from $-2.03(8) \times 10^{-13}$ to $-1.75(6) \times 10^{-13}$ Hz s $^{-1}$ (GögüS et al. 2008, 2010), which corresponds to a relative decrease in $\dot{\nu}$, $\Delta\dot{\nu}/\dot{\nu} \sim -(1.4 \pm 0.4) \times 10^{-1}$. This large and rapid decrease in $\dot{\nu}$ was explained as the effects of timing-noise torque and outbursts (GögüS et al. 2010), instead of as a secular dipole magnetic field decay.

Recently, Dib & Kaspi (2014) presented a summary of the long-term evolution of various properties of five AXPs including 1E 1841 and 1E 2259, regularly monitored with *RXTE* from 1996 to 2012. Influenced by frequent glitches and magnetar outbursts, 1E 1841 and 1E 2259 exhibited large fluctuations in their spin-down parameters ν and $\dot{\nu}$. However, both AXPs obviously exhibited net decrease in $\dot{\nu}$. For AXP 1E 2259, its $\dot{\nu}$ decreased from $-1.020(17) \times 10^{-14}$ to -0.96748×10^{-14} Hz s $^{-1}$ during an interval of MJD 50355–54852 (Dib & Kaspi 2014), which corresponds to $\Delta\dot{\nu}/\dot{\nu} \sim -(5.1 \pm 1.7) \times 10^{-2}$. For AXP 1E 1841, its $\dot{\nu}$ decreased from $-2.9954(7) \times 10^{-14}$ to $-2.944(11) \times 10^{-13}$ Hz s $^{-1}$ during a interval of MJD 51225–55903 (Dib & Kaspi 2014), which corresponds to $\Delta\dot{\nu}/\dot{\nu} \sim -(1.7 \pm 0.4) \times 10^{-2}$.

If the relative decrease in $\dot{\nu}$ of magnetars is due to the decay of their surface dipolar fields, then it would imply the mean surface dipolar field decaying-rates of $dB_p/dt = 2dB_d/dt = -(4.6 \pm 0.8) \times 10^{13}$ G yr $^{-1}$, $-(2.6 \pm 0.8) \times 10^{11}$ G yr $^{-1}$, and $-(7.4 \pm 2.2) \times 10^{11}$ G yr $^{-1}$ for SGR 0501, 1E 2259, and 1E 1841, respectively (for a rotator in vacuum, $B_d \simeq 3.2 \times 10^{32} (-\dot{\nu}/\nu^3)^{1/2}$ G). However, a large field decay-rate of $|dB_d/dt| \geq 10^{11}$ G yr $^{-1}$ for a magnetar is not realistic and contrary to the above sensible estimates, $dB_d/dt \sim -(10^8 - 10^{10})$ G yr $^{-1}$, based on the updated magneto-thermal evolution models by Pons et al. (2012) and Viganò et al. (2013). In a word, an actual decay of magnetospheric torque can explain the obvious decrease in $\dot{\nu}$ and the high braking index for a magnetar, but could result in an over-estimate of the surface dipolar field decay rate.

Many authors (e.g., Harding et al 1999; Spitkovsky 2006; Beskin & Nokhrina 2007; Tasng & Gourgouliatos 2013; Antonopoulou et al. 2015) investigated the external magnetospheric mechanisms that can explain larger decrease in $|\dot{\nu}|$ during the pulsar spin-down. The rotation of a pulsar induces an electric field accelerating charges off the star's surface. The magnetosphere is expected to be filled with cascade plasma, which will screen the electric field along the magnetic field lines (Goldreich & Julian 1969). The magnetospheric current, \vec{J} , flowing in the magnetosphere and closing under the polar-cap surface, provides an additional

braking torque,

$$-\vec{T}_j = \frac{1}{c} \int [\vec{r}, [\vec{J}_s, \vec{B}_p]] dS. \quad (13)$$

This braking torque on the star from the magnetospheric current is comparable to $-T_{\text{MDR}}$, the braking torque on the star for MDR model⁶. From Eq. (13), a decreasing magnetospheric current \vec{J} produces a decaying $-\vec{T}_j$, which will cause a decrease in $\dot{\nu}$. For a net decay of torque due to the decrease in \vec{J} , the relative decrease in the spin-down rate is estimated as $\Delta T_j/T_j \simeq \Delta \dot{\Omega}/\dot{\Omega} = \Delta \dot{\nu}/\dot{\nu}$ assuming the inertial momentum I , and the angle between rotational and magnetic axis, χ are constants. Note that, a precise calculation of $\dot{\Omega}$ (or $\dot{\nu}$) depends on solving the Euler dynamics equations that are very complicate and uncertain (Beskin & Nokhrina 2007).

It is also possible that a decrease in χ can cause a decrease in spin-down rate, as observed. During the long-term observations, these three magnetars with SNRs experienced frequent outbursts and glitches. (Göğüş et al. 2008, 2010; Dib & Kaspi 2014). often accompanied by crust fractures (Thompson et al. 1995, 1996, 2002, Woods et al. 2007). During post-outburst or glitch recoveries, the stellar platelets move towards the rotational axes. The magnetic field lines anchored to the crusts follow the motion, and the inclination angle χ decreases (Antonopoulou et al. 2015). A decrease in χ will result in a net decay of the magnetospheric braking torque. Thus, the overall effect can be a decrease in $\dot{\nu}$. For a small decrease of χ , the relative decrease in $\dot{\nu}$ is estimated as $\Delta T_{\text{dip}}/T_{\text{MDR}} \simeq \Delta \chi/\tan \chi \simeq \Delta \dot{\nu}/\dot{\nu}$ in MDR model, or as $\Delta T_{\text{ff}}/T_{\text{ff}} \simeq \Delta \chi \sin 2\chi / (1 + \sin^2 \chi) \simeq \Delta \dot{\nu}/\dot{\nu}$, here T_{ff} is the braking torque for the force-free magnetosphere⁷ (Spitkovsky 2006; Antonopoulou et al. 2015). If the external magnetospheric mechanisms (whether due to the change in the current or due to the change in the inclination angle) dominate the spin-down evolutions for three magnetars, the order of magnitude of the relative decreases in the braking torque is about $|\Delta T/T| \approx |\Delta \dot{\nu}/\dot{\nu}| \sim 10^{-1} - 10^{-2}$, as observed in 1E 2259, 1E 1841 and SGR 0501.

In summary, we have quantitatively analyzed several physical processes (the decay of surface dipolar field, the decline of the current, and the decrease in the inclination angle), possibly causing $n > 3$ for magnetars. A common characteristic of these processes is that they can result in a decay of the braking torque on the star. Here we ignore the effects of the stellar multipole magnetic moments on the magnetar braking indices, because the higher-order magnetic moments decay rapidly with the distance to stellar center.

⁶ In the simplest approximation for pulsar spin-down in MDR model, the braking torque on the star is $-T_{\text{MDR}} = \frac{B_p^2 R^6 \Omega^3}{6c^3} \sin^2 \chi$, here R is the stellar radius, and χ is the inclination angle, i.e., the angle between rotational and magnetic axis.

⁷ If the magnetosphere is filled with abundant plasma it can be considered in the force-free regime, where the induced electric field along field lines disappears everywhere except in the acceleration zones above polar caps and regions where plasma flow is required, the braking torque on the star, $-T_{\text{ff}} = \frac{B_p^2 R^6 \Omega^3}{6c^3} (1 + \sin^2 \chi)$ (Spitkovsky 2006).

3.3 Case of $1 < n < 3$

In previous works, many authors proposed various models to explain why the observed braking indices of pulsars $1 < n < 3$, e.g., neutrino and photon radiation (Peng et al. 1982); the combination of dipole radiation and the propeller torque applied by debris-disk (Alpar & Baykal 2006; Chen & Li 2006); frequent glitches, as well as magnetosphere currents (Beskin & Nokhrina 2007). In this work, the lower braking indices of $1 < n < 3$ for six magnetars with SNRs are attributed to the combination of MDR and wind-aided braking. Recently, the extended emission observed from 1E 1547 and Swift J1834 are proposed to be magnetism-powered pulsar-wind-nebulas (PWNs), which may accelerate plasma to very high energy and radiate high-energy photons (see Kargaltsev et al. 2012, and references therein). The possible existence of magnetar PWNs lends a potential and direct support to our assumption of wind-aided braking.

With the aid of strong magnetar wind, the closed magnetic-field lines are combed out at the extended Alfvén radius r_A , where the magnetic energy density equals the particle kinetic-energy density. The braking torque resulting from tangential acceleration of outflowing relativistic plasma is $-T_{\text{wind}} \approx \dot{M} \Omega r_A^2$, where \dot{M} is the total mass-loss rate (Manchester et al. 1985). The accelerated outflowing plasma will carry away the star’s angular momentum, and thus the spin-down rate of the magnetar will increase. The added braking torque due to a magnetar wind extends the effective magnetic braking “lever arm” (Thompson et al. 2000), causing the magnetar braking index to decrease, i.e., $n < 3$.

In the scenario of wind-aided braking, the value of the effective braking index n of a magnetar depends on the competition of the magneto-dipole braking torque $-T_{\text{dip}}$ and wind-braking torque $-T_{\text{wind}}$. If $|T_{\text{wind}}| \gg |T_{\text{dip}}|$, the value of n will be close to 1, and if $|T_{\text{dip}}| \gg |T_{\text{wind}}|$, the value of n will be close to 3. Unlike the persistent soft X-ray luminosity of a magnetar L_X , the persistent magnetar wind luminosity L_W cannot be obtained from observations. Moreover, it’s very difficult to determine L_W of a magnetar theoretically, due to the lack of a detailed magnetar-wind mechanism. The well-known magnetar wind-braking model proposed by Harding et al. (1999) implies a braking index of

$$n = 3 - \frac{2\nu}{|\dot{\nu}|} \frac{L_W^{1/2} B_d R^3}{2I\sqrt{6c^3}}, \quad (14)$$

where we employ standard values of $R = 10\text{km}$ and moment of inertia $I = 10^{45} \text{g cm}^2$. Note that, by definition, the inferred value of n is always within the range of 1~3. In the above expression, n is an effective braking index, thus L_W is the effective wind-luminosity, and B_d is the effective surface dipolar field. However, due to lack of the detailed information of the effective n , B_d and L_W , the importance of Eq.(14) has not been recognized in previous works. From the above expression, the magnetar wind luminosity can be estimated as

$$L_W \simeq \frac{6(3-n)^2 \dot{\nu}^2 I^2 c^3}{\nu^2 B_d^4 R^6}. \quad (15)$$

By using Eq.(15), we estimated possible wind luminosity of magnetars, L_W , as listed in Table 5. Here we assume that

Table 5. The relations among L_{rot} , L_X and L_W of magnetars with different braking indices. Six sources in the upper part of Table 5 have braking indices $1 < n < 3$, while three sources in the lower part have braking indices $n > 3$. All the date $L_X(2\text{-}10\text{ keV})$ are cited from McGill SGR/AXP Online Catalogue. The rotation-energy loss rate is calculated by $L_{\text{rot}} = 4\pi^2 I \nu \dot{\nu}$, here $I = 10^{45} \text{ g cm}^2$.

Name	L_{rot} (erg s $^{-1}$)	L_X (erg s $^{-1}$)	L_W (erg s $^{-1}$)	L_W/L_{rot}	L_W/L_X	L_X/L_{rot}
SGR 1627*	$4.3(9) \times 10^{34}$	3.6×10^{33}	$(2.304 \pm 0.997) \times 10^{35}$	5.36 ± 2.32	6.40 ± 2.77	0.84 ± 0.17
Swift J1834*	2.1×10^{34}	$< 0.84 \times 10^{31}$	$(3.157 \pm 0.165) \times 10^{35}$	15.03 ± 0.78	37583.3 ± 1964.3	< 0.0004
1E 1547	2.11×10^{35}	1.3×10^{33}	$(1.278 \pm 0.097) \times 10^{36}$	6.22 ± 0.46	1009.2 ± 75.4	0.0063
---†	1.032×10^{35}	1.3×10^{33}	$(8.92 \pm 3.71) \times 10^{34}$	0.86 ± 0.36	68.6 ± 28.6	0.013
---†	$1.20(18) \times 10^{35}$	1.3×10^{33}	$(2.40 \pm 1.71) \times 10^{35}$	1.98 ± 1.21	184.4 ± 131.5	0.011(2)
---†	$2.76 \pm 1.58 \times 10^{35}$	1.3×10^{33}	$(2.43 \pm 2.05) \times 10^{35}$	7.43 ± 5.21	1867.7 ± 1576.8	0.0047(29)
CXOU J1714	4.51×10^{34}	5.6×10^{34}	$(1.53 \pm 1.52) \times 10^{35}$	3.38 ± 3.37	2.72 ± 2.71	1.302
---†	4.15×10^{34}	5.6×10^{34}	$(1.15 \pm 1.57) \times 10^{35}$	2.70 ± 3.78	2.05 ± 2.80	1.35
---†	$7.41(35) \times 10^{34}$	5.6×10^{34}	$(5.36 \pm 4.26) \times 10^{35}$	7.23 ± 5.75	12.9 ± 10.2	0.756
SGR 0526	$2.87(7) \times 10^{33}$	1.89×10^{35}	$(4.13 \pm 0.55) \times 10^{33}$	1.44 ± 0.19	0.023 ± 0.003	65.8 ± 1.5
---†	$4.9(4) \times 10^{33}$	1.89×10^{35}	$(2.75 \pm 0.53) \times 10^{34}$	5.61 ± 1.17	0.146 ± 0.028	38.6 ± 2.7
PSR J1622	$8.3(5) \times 10^{33}$	4.4×10^{32}	$(1.47 \pm 0.40) \times 10^{34}$	1.77 ± 0.49	33.4 ± 9.0	0.053(3)
---†	$(7.0 \pm 2.4) \times 10^{33}$	4.4×10^{32}	$(4.87 \pm 4.13) \times 10^{33}$	0.69 ± 0.58	11.1 ± 9.4	0.063(21)
1E 2259+586	5.6×10^{31}	1.7×10^{34}	303.57
1E 1841-045	9.9×10^{32}	1.84×10^{35}	185.85
SGR 0501+4516	1.2×10^{33}	8.1×10^{32}	5.33

Footnote:* According to the “fundamental plane”(Rea et al. 2012) for radio magnetars with $L_{\text{rot}} > L_X$, this source should have radio emission, however no radio emission was reported to date.

the effective value of surface dipolar field to be the observed value of B_d for convenience. From Table 5, the value of L_X is obviously unrelated to that of L_{rot} , this is because magnetar X-ray emission is powered by magnetic field free energy. With the exception of SGR 0526, magnetars’ wind luminosities are bigger than their soft X-ray luminosities. Since the magnetar wind is universally believed to be powered by the decay of its superhigh internal magnetic field (e.g., Woods et al 1999; Thomspon et al. 2002 Potekhin & Lai 2007; Tiengo et al. 2013), our estimations of L_W suggest that a magnetar should possess a strong external magnetic field, as well as a strong internal magnetic filed. In addition, we plot the diagram of L_W/L_{rot} vs. n for six magnetars. Fig.2 shows a weak anti-correlation between L_W/L_{rot} and n : the higher the ratio of L_W/L_{rot} , the lower n becomes. If the wind braking dominates over magnetic- dipole braking, then $n \sim 1$. Notice that even in the scenario of wind-aided braking, a magnetar is still experiencing a normal magnetic-field decay with a very low field decay-rate of \dot{B}_d . In the same way, even if the surface dipolar field decay dominates, the spin-down of a magnetar is still affected by its wind braking torque. In this case, compared with the spin-down luminosity L_{rot} , the wind luminosity L_W is too small to be considered in this work.

In addition, SGR 0501 possesses a relatively large ratio of $L_X/L_{\text{rot}} \sim 5.3$ (see in Table 5), which is higher than those of all magnetars (except for SGR 0526 with $1 < n < 3$. The large ratio of L_X/L_{rot} could be served as a strong hint of surface dipolar field decay for this source. Recently, Tong et al. (2013) proposed a multipole field-powered wind model for magnetars. The authors assumed that all the high luminosity magnetars with $L_X > L_{\text{rot}}$ spin down via wind

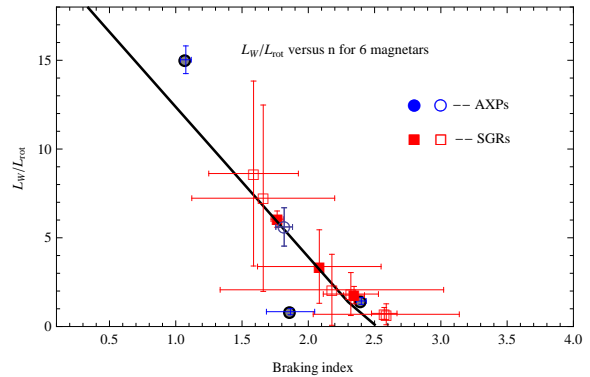


Figure 2. L_W/L_{rot} versus n for six magnetars. Blue circles and red squares represent SGRs and AXPs, respectively. Data for empty circles and squares are from Table 3.

braking, and transient magnetars (including PSR J1622, 1E 1547 and SGR 1627) with $L_X < L_{\text{rot}}$ spin down via magnetic dipole braking. Based on a simple assumption of $L_W = L_P = 10^{35} \text{ erg s}^{-1}$ (L_P is the escaping particle luminosity). They concluded that, for typical AXPs and SGRs, the dipole magnetic field in the case of wind braking is about ten-times lower than that of magnetic- dipole braking, and a strong dipole magnetic field may be no longer necessary for some sources and so on. However, when estimating B_d , Tong et al.(2013) didn’t take into account effective braking indices. Their simple assumptions of uniform “wind braking” and “magnetic dipole braking” may not be supported by a range of $n \sim 1 \sim 41$ provided in this work. Additionally, a magnetar’ wind energy and soft X-ray energy are two

distinct forms of energy, the former refers to the particle kinetic-energy, while the latter refers to the photon-energy, though they could come from “same energy reservoir” (Tong et al. 2013).

4 A POTENTIAL APPLICATION OF OUR MODEL

Recently, AXP 1E 2259 clearly showed a sudden spin-down, which was a so-called anti-glitch (Archibald et al. 2013). The authors proposed two possible timing models explaining the observational phenomenon: (i) one anti-glitch followed by a normal glitch after ~ 100 d or (ii) two anti-glitches separated by ~ 50 d. Despite the discrepancies in the timing parameters for both models, there was a net decrease in ν , $\Delta\nu = -2.06(8) \times 10^{-7}$ Hz ($\Delta\nu/\nu = -1.44(6) \times 10^{-7}$) and a remarkable increase in $|\dot{\nu}|$, $\Delta\dot{\nu} = -1.3(4) \times 10^{-7}$ Hz s $^{-1}$ during anti-glitch epoch, where ν , and $\dot{\nu}$ are the spin frequency, and its derivative before the anti-glitch, respectively.

Another important aspect for the anti-glitch event is an increase by a factor 2 in the soft X-ray (2–10 keV) luminosity of 1E 2259 (Archibald et al. 2013). The energy spectrum of this source became harder, and its flux decreased in a power-law form. On 2012 April 21, a short burst with a duration of 36 ms was observed by *Fermi*/Gamma-ray Burst Monitor (GBM).

There are several explanations for the anti-glitch, which are based on either external (e.g., Lyuticov 2013; Katz 2014; Tong 2014; Huang & Geng 2014) or on internal (e.g., Duncan 2013; García & Ranea-Sandoval 2015) origins. However, these authors either avoided discussing the star’s braking index n or treated it as a constant, (i.e., ignored the variation of n at the anti-glitch) when constructing their theoretic models.

As to the external origin of the anti-glitch, in order to account for enhanced spin-down and spectral hardening, Lyutikov (2013) assumed a sudden twisting of the magnetic field lines in magnetosphere with an increased twist angle of $\Delta\phi \sim 0.37$ rad; Tong (2014) assumed an increased particle wind with luminosity $L_W \sim 10^{35}$ erg s $^{-1}$ (which is higher than its persistent soft X-ray luminosity $L_X \sim 1.7 \times 10^{34}$ erg s $^{-1}$); and Katz (2014) assumed an increased accretion of residual matter with the opposite sense of angular momentum and a total accretion mass $\Delta M \sim 10^{21}$ g at the anti-glitch epoch. The subsequent observation of $\dot{\nu}$ and no detection of surrounding afterglow at radio and X-ray wavelengths argued against the wind model, the accretion model and the twisted magnetosphere model, as mentioned in Archibald et al. (2013) and García & Ranea-Sandoval (2015).

In the above external origin models, the chosen braking indices are in the same way in the range of $1 < n < 3$, because an additional braking torque significantly influences the star’s spin-down before the anti-glitch, but there are no discussions on variations in the braking index at the anti-glitch have not yet appeared. However, a low braking index $1 < n < 3$ cannot account for the large age-discrepancy between τ_c and t_{SNR} for this source ($\tau_c = 230$ kyrs, and $t_{\text{SNR}} = (15 \pm 5)$ kyrs), as estimated from Eq. (7). The measured braking index, $n = 31.50 \pm 10.17$ in this work does not support the proposed models.

We propose that the other external mechanisms (e.g., magnetospheric torque’s increase due to the increase in the inclination angle, or in the surface dipolar magnetic field) may operate in this anti-glitch event. For example, a net decrease in B_d (or in χ or in magnetospheric current-density J_s) in a long timescale can result in the higher braking index $n = 31.50 \pm 10.17$ for 1E 2259, as discussed in Sec. 3.2, however, an abrupt increase in any of quantities above (this is possible) could not only account for the anti-glitch event, but also result in a decrease in n due to a sudden increase in the magnetospheric braking torque. We can estimate the value of Δn at the anti-glitch as following:

(i) As pointed out in Viganò (2013), the parameter K in Eq.(1) for a magnetic process is approximately considered as a constant, if ignoring an additional braking torque on the star due to strong particle wind, or due to strong accretion of matter with opposite sense of angular momentum, or due to strongly twisted magnetosphere.

(ii) According to Eq. (1), the star’s spin-down before the anti-glitch is written as $\Omega_{\text{bef}} = -K\Omega_{\text{bef}}^n$, and the star’s spin-down during the anti-glitch is written as $\dot{\Omega}_{\text{anti}} = -K\Omega_{\text{anti}}^{n+\Delta n}$. We also assume $\Omega_{\text{bef}} \simeq \Omega_{\text{anti}} = \Omega = 2\pi\nu$, because $\Delta\Omega/\Omega = \Delta\nu/\nu = -1.44(6) \times 10^{-7}$, here ν is the spin frequency before the anti-glitch. Then we get an approximation relation, $\dot{\Omega}_{\text{anti}}/\dot{\Omega}_{\text{bef}} = \dot{\nu}_{\text{anti}}/\dot{\nu}_{\text{bef}} \simeq (2\pi\nu)^{n+\Delta n}/(2\pi\nu)^n = (2\pi\nu)^{\Delta n}$.

(iii) The variation of Δn at the anti-glitch is estimated as

$$\Delta n = \ln\left(\frac{\dot{\nu} + \Delta\dot{\nu}}{\dot{\nu}}\right)/\ln(2\pi\nu). \quad (16)$$

Inserting $\nu = 0.143285110(4)$, $\dot{\nu} = -9.80(9) \times 10^{-15}$ Hz s $^{-1}$ and $\Delta\dot{\nu} = -1.3(4) \times 10^{-7}$ Hz s $^{-1}$ the values of ν , $\dot{\nu}$, and $\Delta\dot{\nu}$ of 1E 2259 into the above equation yields $\Delta n \sim -(1.1 \pm 0.3)$, which corresponding to a relative decrease in n , $\Delta n/n \sim -(3.5 \pm 1.5) \times 10^{-2}$.

In other words, one should take into account the braking index and its variation during the anti-glitch in the external mechanisms for the origin of the anti-glitch.

For the internal origin of the anti-glitch, Duncan (2013) assumed that the stellar superfluid rotates more slowly than the crust, and a sudden instability by which vortices shift inward, would quickly spin up the superfluid, then the rest of the star spin down due to angular-momentum conservation. However, this model didn’t give some observational predictions, due to a lack of a quantitative description.

Very recently, García & Ranea-Sandoval (2015) attributed the anti-glitch to a sudden change in the stellar structure. Their picture is the following: given an initial strong toroidal magnetic field B_t^i , the star’s crust crystallizes in a prolate equilibrium configuration. As a consequence of the long-term decay of the internal magnetic field, an initially prolate configuration departs more and more from equilibrium until it reaches a critical strain cracking the stellar crust. The subsequent re-accommodation of the star into a stable, more spherical shape leads to the observed sudden frequency spin-down. The internal field decay due to the combination Ohmic and Hall effects (García & Ranea-Sandoval 2015) may actually account for the measured high braking index of 1E 2259. However, the authors did not explain the variation of $\Delta\dot{\nu}$ because they ignored any external braking torque. Actually, it is very hard to ensure angular momentum conservation according to the estimations of the

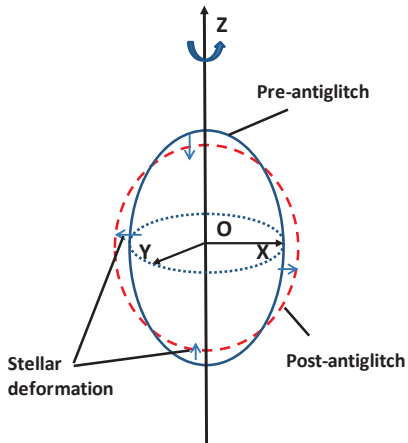


Figure 3. The structure deformation of a magnetar with super-high internal toroidal magnetic field during anti-glitch epoch.

variation of ΔB_t . Suppose that if the star experienced a sudden decay of B_t with the order of magnitude, $\Delta B_t \sim$ several times 10^{14} G the magnetic flux’s motion via Hall drift could result in an increase in the surface dipolar magnetic field (despite that it is experiencing a long-term decay), which could cause an increase in the dipolar braking torque, then the star could slow more slowly than that estimated by a simple angular momentum conservation. Maybe the value of ΔB_t was over-estimated base on angular momentum conservation in the model of García & Ranea-Sandoval (2015).

Based on the estimated value of n of 1E 2259 and its timing parameters before and at the anti-glitch, we have discussed the feasibility of various models proposed. Here our main aim is to remind that there could be some connections between the magnetar’s anti-glitch and its braking index, and the braking index should be considered and treated correctly when explaining the anti-glitch.

5 SUMMARY AND DISCUSSION

We have presented the constrained values for magnetar braking indexes, n , by using the possible magnetar–SNR associations, and discussed the possible origins and application of the braking indices. Our main conclusions are as follows.

(i) Based on possible timing solutions of magnetars and updated measurements of their SNRs, we estimate the braking indices n of nine magnetars with SNRs. The constrained values of n are found to cluster in a range of $n \sim 1 - 41$.

(ii) We attribute the higher braking indices, $n > 3$, of 1E 2259, 1E 1841 and SGR 0501 to the surface dipolar field decay, or to the decay of external magnetospheric braking torque. In the former case, the estimated dipolar field decay rates, based on the updated magneto-thermal evolution models, are comparable to the measured values of n for these three sources.

(iii) We attribute the lower braking indices, $1 < n < 3$, of other six magnetars (SGR 0526, SGR 1627, PSR J1622,

CXOU J1714, Swift J1734 and 1E 1547) to a combination of MDR and wind-aided braking, and estimate the possible wind luminosities L_W . According to our estimations, magnetars should possess both strong internal and external magnetic fields. We find a weak anti-correlation between L_W/L_{rot} and n for magnetars with $1 < n < 3$.

(iv) Based on the measured value of n of 1E 2259 and its timing parameters before and at the anti-glitch, we briefly review and discuss current theoretic models proposed for the anti-glitch in 1E 2259. We proposed that anti-glitch and the braking index are closely related, and the braking index should be considered and treated correctly if one try to explain the anti-glitch event.

In this work, we remind that, in order to derive an analytical expression for estimating the magnetar’s true age, the braking index is assumed to be a constant. However, the inferred quantities (e.g., B_d and τ_c) of a magnetar strongly depend on the current values of P and \dot{P} (or of ν and $\dot{\nu}$) that will vary with time. There always exist observational errors when estimating t_{SNR} for magnetars. Thus, for some sources, their constrained values of n are subject to substantial uncertainties, and will be modified with future observations.

The resulting values of n for magnetars may be useful for investigations of the magnetar radio emission during outbursts and the anti-glitch events. We believe that more observations of magnetars and their SNRs will help in further constraining the magnetar braking mechanisms.

ACKNOWLEDGMENTS

We thank anonymous referees for carefully reading the manuscript and providing valuable comments that improved this paper substantially. We also thank Prof. Yang Chen for useable suggestions and Dr. Rai Yuen for smoothing out the language. This work was supported by Xinjiang Natural Science Foundation No.2013211A053. This work is also supported in part by Chinese National Science Foundation through grants No.11173041, 11003034, 11273051, 11373006 and 11133001, National Basic Research Program of China grants 973 Programs 2012CB821801, the Strategic Priority Research Program “The Emergence of Cosmological Structures” of Chinese Academy of Sciences through No.XDB09000000, the West Light Foundation of Chinese Academy of Sciences No.2172201302, and by a research fund from the Qinglan project of Jiangsu Province.

REFERENCES

- Aguilera D. N., et al., 2008, *A& A*, 486, 255
- Aharonian F., et al., 2008, *A& A*, 486, 829
- Alpar M. A., Baykal A., 2006, *MNRAS*, 372, 489
- Anderson G. E., et al., 2012, *ApJ*, 751, 53
- Antonopoulou D., et al., 2015, *MNRAS*, 447, 3924
- Archibald R. F., et al., 2013, *Nature*, 497, 591
- Archibald R. F., et al., 2014, *arXiv.1412.2789*
- Badenes C., et al., 2009, *ApJ*, 700, 727
- Bandiera R., 1984, *A& A*, 139, 368
- Barsukov D. P., Tsygan A. I., 2010, *MNRAS*, 409, 1077
- Barthelmy S. D., et al., 2008, *GCN Circ*, 8113**
- Beskin V. S., Nokhrina E. E., 2007, *ApSS*, 308, 569

- Biryukov A., et al., 2012, MNRAS, 420, 103
 Camilo F., et al., 2007, ApJ, 666, L93
 Camilo F., et al., 2008, ApJ, 679, 681
 Castro D., et al. 2012, ApJ, 756, 88
 Caswell J. L., et al. 1975, A&A, 45, 239
 Chen W. C., Li X. D., 2006, A&A, 450, L1
 Cioffi D. F., et al., 1988, ApJ, 334, 252
 Clark, D. H., Stephenson, F. R., 1975, The Observatory, 95, 190
 Corbel S., et al., 1999, ApJ, 526, L29
 Cordes, J. M., Lazio, T. J. W., 2002, arXiv:astro-ph/0207156
 Cox D., 1972, ApJ, 178, 159
 Dib R., Kaspi V. M., Scholz P., et al., 2012, ApJ, 748, 3
 Downes A., et al., 1984, MNRAS, 210, 845
 Dib R., Kaspi V. M., 2014, ApJ, 784, 37
 Duncan R. C., Thompson C., 1992, ApJ, 392, L9
 Duncan R. C., 2013, Nature, 497, 574
 Durant M., van Kerkwijk M H., 2006, ApJ, 650, 1070
 Ellison D. C., et al., 2007, ApJ, 661, 879
 Espinoza C. M., et al., 2009a, ApJ, 690, L105
 Espinoza C. M., et al., 2009b, MNRAS, 399, L44
 Espinoza C. M., et al., 2011, ApJ, 741, L13
 Espinoza C. M., 2013, IAU Symposium, Vol.291, p.195, ed: J. van Leeuwen (Cambridge University Press)
 Evans W. D., et al., 1980, ApJ, 237, L7
 Fahlman G. G., Gregory P. C., 1981, Nature, 293, 202
 Gaensler B. M., et al., 1999, ApJ, 526, L37
 Gaensler B. M., et al., 2001, ApJ, 559, 963
 Gaensler B. M., 2004, Adv. Space. Res. 33, 645
 Gaensler B. M., & Slane P. O., 2006, Annu. Rev. Astro. Astrophys. 44, 14
 Gaensler B. M., Chatterjee S., 2008, GCN Circ, 4189, 1
 Gaensler B. M., 2014, GCN Circ, 16533
 García F., Ranea-Sandoval I F., 2015, MNRAS, 449, L73
 Geppert P., Rheinhardt M., 2002, A&A, 392, 1015
 Gao Z. F., et al. 2011, Ap&SS, 332, 129
 Gao Z. F., et al., 2012, Chin. Phys. B 21(5), 057109
 Gao Z. F., et al., 2013, Mod. Phys. Lett. A, 28(36), 1350138
 Gelfand J. D., Gaensler B. M., 2007, ApJ, 667, 1111
 Göğüş E., et al., 2008, ATel, 1677, 1
Göğüş E., et al., 2010, ApJ, 722, 899
Goldreich P., Julian W. H., 1969, ApJ, 157, 869
 Gotthelf E. V., Vasisht G., 1997, ApJ, 486, L133
 Halfand D. J., et al., 1994, ApJ, 434, 627
 Halpern J. P., Gotthelf E. V., 2010a, ApJ, 710, 941
 Halpern J. P., Gotthelf E. V., 2010b, ApJ, 725, 1384
 Harding A. K., et al., 1999, ApJ, 525, L125
 Haskell B., Melatos A., 2015, Int.J.Phys.D 24,153008
Ho W. C. G., 2011, MNRAS, 414, 2567
 Hobbs G., et al., 2010, MNRAS, 402, 1027
 Horvath J. E., Allen M. D., 2011, RAA, 11, 625
 Huang Y. F., Geng J. J., ApJ 782, L20
 Hurley K., et al., 1999, ApJ, 510, L107
 Kargaltsev O., et al., 2012, ApJ, 748, 26
 Katz J I., 2014, ApSS. 349, 611
 Klose S., et al., 2004, ApJ, 609, L13
 Kothes R., et al., 2002, ApJ, 576, 169
 Kothes R., Foster T., 2012, ApJ, 746, L4
 Kou F F., Tong H., 2015, MNRAS, 450, 1990
 Kouveliotou C., et al., 1994, Nature, 368, 125
 Kutukcu P., Ankey A., 2014, Int. J.Phys.D. 23, 1450083
 Kulkarni S. R., et al., 2003, ApJ, 585, 945
 Lai X. Y., Gao C. Y., Xu R. X., 2013, MNRAS, 431, 3290
 Leahy D. A., Aschenbach B., 1995, A&A, 293, 853
 Leahy D. A., Tian W. W., 2007, A&A, 461, 1013
 Levin L., et al., 2010, ApJ, 721, L33
 Livingstone M. A., et al., 2007, ApSS, 308, 317
 Lyne A. G., et al., 1993, MNRAS, 265, 1003
 Lyne A. G., et al., 1996, Nature, 381, 497
 Lyutikov M., 2013, arXiv:1306.2264
 Magalhaes N. S., et al., 2012, ApJ, 755, 54
 Manchester R. N., Taylor J. H., 1977, Pulsars (W. H. Freeman & Co Ltd)
 Manchester R. N., et al., 1985, Nature, 313, 374
 Manchester R. N., et al., 2005, AJ, 129, 1993
 Mereghetti S., 2008, Astron. Astrophys. Rev. 15, 225
 Middleditch J., et al., 2006, ApJ, 652, 1531
 Muslimov A., Page D., 1995, ApJ, 440, L77
 Nakamura R., et al., 2009, PASJ, 61, 5197
 Olausen S. A., Kaspi V. M., 2014, ApJS, 212, 6
 Ostriker J.P., McKee C.F., 1988, Rev. Mod. Phys. 60, 1
 Park S., et al., 2012, ApJ, 748, 117
 Peng Q. H., et al., 1982, A&A, 107, 258
 Pons J. A., Geppert U., 2007, A&A, 470, 303
 Pons J. A., Miralles J. A., Geppert U., 2007, A&A, 496, 207
 Pons J. A., Viganò D., Geppert U., 2012, A&A, 547, A9
 Potekhin A. Y., Lai D., 2007, MNRAS, 376, 793
 Rea N., et al., 2012, ApJ, 748, L12
 Romer A. K., et al., 2001, ApJ, 547, 594
 Roy J., et al., 2012, MNRAS, 424, 2213
 Sarma, A., et al., 1997, ApJ, 483, 335
 Sasaki M., et al., 2004, ApJ, 617, 322
 Sasaki M., et al., 2013, ApJ, 552, 45
 Sato T., et al., 2010, PASJ, 62, L33
 Sedov L. I., 1946, Dokl. Akad. Nauk SSSR, 42, 17
 Sedov L. I., 1959, Similarity and Dimensional Methods in Mechanics, Academic Press, New York
 Smith D. A., et al., 1999, ApJ, 519, L147
 Spitkovsky A., 2006, ApJ, 648, L51
 Taylor G., 1950, Proc.R.Soc. London. A, 201, 159
 Tendulkar S. P., et al., 2012, ApJ, 761, 76
 Tendulkar S. P., et al., 2013, ApJ, 771, 11
 Thompson C., Duncan R. C., 1995, MNRAS, 275, 255
 Thompson C., Duncan R. C., 1996, ApJ, 473, 322
 Thompson C., et al., 2000, ApJ, 543, 340
 Thompson C., et al., 2002, ApJ, 561, 980
 Tian W. W., Leahy D. A., 2008, ApJ, 677, 292
 Tian W. W., et al., 2007, ApJ, 657, L25
 Tian W. W., et al., 2010, MNRAS, 404, L1
 Tian W. W., Leahy D. A., 2012, MNRAS, 421, 2593
 Tiengo A., et al., 2009, MNRAS, 399, L74
 Tiengo A., et al., 2010, ApJ, 710, 227
 Tiengo A., et al., 2013, Nature, 500, L312
 Tong H., et al., 2013, ApJ, 768, 144
 Tong H., 2014, ApJ, 784, 86
 Truelove J.K., McKee C.F., 1999, ApJS, 120, 299
 Tsang D., Gourgouliatos K., 2013, ApJ, 773, L17
 Vasisht G., Gotthelf E. V., 1997, ApJ, 486, L129
 Vink J., Kuiper L., 2006, MNRAS, 370, L370
 Viganò D., Pons J. A., Miralles J. A., 2012, CoPhC, 183, 2042
 Viganò D., Pons J. A., 2012, MNRAS, 425, 2487

- Viganò D., Rea N., Pons J. A., et al., 2013, MNRAS, 434, 123
- Viganò D., 2013, Ph.D. Thesis. “Magnetic Fields in Neutron Stars”, Supervisors: Profs. Pons J. A., and Miralles J. A., arXiv:1310.1243
- Weltevrede P., et al., 2011, MNRAS, 411, 1917
- White R., Long K., 1991, ApJ, 373, 543
- Woltjer L., 1972, Anu. Rev. Astron. Astrophys. 10129, 463
- Woods P. M., et al., 1999, ApJ, 518, L103
- Woods P. M., et al., 2007, ApJ, 654, 470
- Yuan J. P., et al., 2010, ApJ, 719, L111
- Xu R. X., 2007, Advances in Space Research, 40, 1453
- Zhang S.-N., Xie Y., 2012, ApJ, 761, 102
- Zhang S.-N., Xie Y., 2013, Int. J. Mod. Phys.D., 22, 1360012
- Zheng X. P., Yu Y. W., Li J. R., 2006, MNRAS, 369, 376
- Zhou P., et al. 2014, ApJ, 781, L16